

# Uplink Receiver with V-BLAST and Practical Considerations for Massive MIMO System

Li Tian<sup>1</sup>

<sup>1</sup> Department of Electrical and Computer Engineering,  
University of Auckland,  
Auckland, New Zealand

## Abstract

**Abstract**—Massive multiple-input multiple-output (MIMO) systems equipped one base station (BS) with a large number of antenna arrays and allows for improvement on energy and spectral efficiency with the presence of linear signal processing. This paper first explores the fundamental models of massive MIMO from information theoretical perspective, then gives a deep insight of two linear precoders implemented (ZF and MMSE) and optimal ordering algorithm (V-BLAST). Performance analysis on the different precoding methodologies with respect to energy efficiency is provided with proper simulation. Besides, the inter-cell interference due to non-orthogonal pilot sequences in time-duplex division (TDD), or pilot contamination, is discussed after the simulation with current mitigation techniques. Lastly, the generalized issues such as hardware impairments are investigated in terms of their effect on massive MIMO system.

**Keywords**—Energy efficiency; massive MIMO systems; zero forcing; MMSE; V-BLAST; pilot contamination; hardware impairments

## 1. Introduction

MIMO (multiple-input-multiple-output) system has been extensively studied for last two decades. In recent years, multi-user MIMO (MU-MIMO) has been incorporated into many wireless communication standards like LTE and 802.16 (WiMAX). While conventional MIMO focuses on point-to-point links, MU-MIMO enables multiple antennas on a base station (BS) to simultaneously communicate with a set of single-antenna users and share the multiplexing gain among users. In practical implementations, the number of antennas employed by one BS is usually less than 10, thus the relative improvement on spectral efficiency is modest.

A recent proposed massive MIMO system is studied to achieve higher gains and simplify relative signal

processing, as illustrated in Fig. 1. Each BS in a massive MIMO systems employs a higher order of magnitudes, e.g., typically 100 antennas or more. The asymptotic argument of random matrix theory contributes to the transition from random channel matrix distribution to approximate deterministic functions [1]. The transition arises from the elimination of uncorrelated noise and small-scale fading in massive MIMO system, and as the number of antennas of each BS approaches infinity, the transmitted energy required per bit goes to zero. In addition, matrix operations like inversions can be worked out fast with large dimensions of antennas. Thus, simple linear processing methods, such as MRC (maximum ratio combining) for uplink and MRT (maximum ratio transmission) for downlink can be optimal.

This paper firstly reviews the fundamentals of massive MIMO from the information theoretical perspective. In Section 3, different linear precoding strategies are investigated. Apart from conventional matched filtering precoder, ZF (zero forcing) and MMSE (minimum mean-squared error) are studied with the presence of V-BLAST (vertical Bell Laboratories layered space-time) algorithm or optimal ordering. The precoding schemes are discussed under both single-cell and multi-cell processing conditions. Section 4 gives an insight into energy efficiency for different precoding schemes and discussion on complexity of each system. In practice, the transmit power for each antenna are unequal rather than assumed in Section 4. Therefore, Section 5 will give an insight into how the optimal resource allocation strategy is determined on one BS and its effect on energy efficiency. Extensions and generalized issues to consider for a practical system, such as hardware impairments and resulting pilot contamination, will be discussed in Section 5. Research outcomes in massive MIMO and conclusions will be discussed in Section 6.

## 2. Information theory of massive MIMO

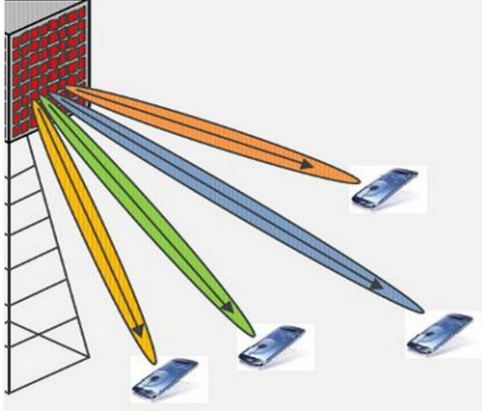


Figure 1: Illustration of Massive MIMO System

This section starts with point-to-point MIMO system from information theoretical perspective, and then discuss the fundamentals of MU-MIMO system with a large number of antennas on one BS links to multiple single-antenna user terminals.

### 2.1 Point-to-Point MIMO

Consider an uplink system with  $N_r$  receive antennas equipped in one BS and  $N_t$  single-antenna equipment. The received vector,  $y \in \mathbb{C}^{N_r}$  can be defined according to [4] [8] as

$$y = \sqrt{\rho}Hx + n \quad (1)$$

Where  $H$  is a  $N_r \times N_t$  deterministic and constant channel matrix,  $x \in \mathbb{C}^{N_t}$  is the transmitted signal vector and  $n \in \mathbb{C}^{N_r}$  stands for noise and interference. The transmit signals are assumed as independent and identically distributed (i.i.d.) Gaussian signal with normalized power, where  $E\{|x|^2\} = 1$ . Noise vector satisfy same conditions with zero-mean symmetrical complex Gaussian elements and identity covariance matrix  $\mathbf{I}$ , thus  $E\{|n|^2\} = \rho^2 = 1$  and  $n \sim \mathcal{CN}(0,1)$ .

If perfect channel state information (CSI) is assumed known in receiver, then according to Shannon's information theory, the instantaneous achievable rate measured in bits-per-symbol can be expressed as

$$C = \log_2 \det(I_{N_r} + \frac{\rho}{N_t} HH^H) \quad (2)$$

Where  $I_{N_r}$  denotes the identity covariance matrix for noise vector and the subscript  $H$  represents Hermitian transpose. The resulting achievable rate  $C$  can be approached by setting transmitter rate with

acceptable outage probability. During signal propagation, since channel matrix  $H$  is normalized, trace  $Tr$  can be used to constrain the bounds of the capacity, where  $Tr(HH^H) \approx N_t N_r$ . Then for point-to-point MIMO with one antenna at each terminal of the link, the upper and lower limits of the capacity are derived in [2][3] as

$$\log_2(1 + \rho N_r) \leq C \leq \min(N_t, N_r) \cdot \log_2(1 + \frac{\rho \max(N_t, N_r)}{N_t}) \quad (3)$$

The lower bound in (3) occurs when only one of the singular values is zero and higher bound in (3) is achieved when all singular values are equal. In practice, the worst case with lowest rate can be obtained when individual elements in either transmit or receive array are irresolvable under line-of-sight (LOS) propagation conditions; the highest rate can be approached with a channel matrix where all propagation coefficients are i.i.d..

Two limiting cases are discussed below, where either number of transmit antennas or receive antennas approaches infinity. For a massive MIMO, the number of receive antennas is much higher than transmit antennas in uplink and vice versa in downlink. Hence when  $N_t \gg N_r$  and assuming the row vectors of  $H$  are orthogonal asymptotically, the achievable rate can be approximated as

$$C_{N_t \gg N_r} \approx N_r \cdot \log_2(1 + \rho) \quad (4)$$

Similarly when  $N_r \gg N_t$

$$C_{N_r \gg N_t} \approx N_t \cdot \log_2(1 + \frac{\rho N_r}{N_t}) \quad (5)$$

### 2.2 MU-MIMO

The favorable propagation in MU-MIMO is achieved when channel matrix  $H$  is i.i.d., and the number of antennas on one BS ( $M$ ) is much larger than number of users ( $K$ ). Under favorable propagation when  $M \gg K$  from [4]

$$\frac{G^H G}{M} \approx \begin{bmatrix} \beta_1 & 0 & \dots & 0 \\ 0 & \beta_2 & \ddots & \vdots \\ \vdots & \ddots & \ddots & 0 \\ 0 & \dots & 0 & \beta_K \end{bmatrix} \triangleq D \quad (6)$$

Where  $G \in \mathbb{C}^{M \times K}$  denotes the reverse link of propagation matrix for small-scale fading,  $D \in \mathbb{C}^{K \times K}$  is a diagonal matrix which accounts for large scale fading coefficients  $\beta$  such as path loss and

shadowing. With the inclusion of channel matrix  $\mathbf{H}$ ,  $G$  can be defined as in [3]

$$G = \mathbf{H}D_{\beta}^{1/2} \quad (7)$$

Hence, to consider with single-cell systems, the product of channel matrix in (2) can be expressed as

$$\mathbf{H}^H \mathbf{H} = D^{1/2} G^H G D^{1/2} \approx M D_{\beta}^{-1} I_K D_{\beta}^{-1} = M D_{\beta} \quad (8)$$

As  $M$  approaches infinity, the column vectors of channel matrix for different users are orthogonal asymptotically. Then for uplink transmission, substitute (8) into (2) and obtain the sum rate where the subscript  $u$  denotes uplink:

$$C \approx \log_2 \det(I_K + M \rho_u D) = \sum_{k=1}^K \log_2 (1 + M \rho_u \beta_k) \quad (9)$$

With orthogonal column vectors and favorable propagation, the matched filter (MF) processing can be employed by BS received signals. Conjugate transpose of the channel matrix is multiplied by receive signal to perform MF processing:

$$\mathbf{H}^H y_u = \mathbf{H}^H (\sqrt{\rho_u} \mathbf{H} x_u + n_u) \approx M \sqrt{\rho_u} D_{\beta} + \mathbf{H}^H n_u \quad (10)$$

The MF processing distributes the signals received from different users into individual streams. For a  $k$ th user, signal to noise ratio (SNR) in (10) is  $M \rho \beta_k$ , which is same as the achievable rate in (9). Since the approximations in (9) and (10) are obtained when the number of antennas on one BS approaches to infinity, simple MF processing is indicated as optimal at the BS with the law of large numbers. With the constraint on BS antenna numbers, more accurate linear precoder or detector are employed by BS and will be discussed in Section 3.

### 3. Precoding

Conventional MIMO systems can use either non-linear or linear precoding methodologies. Because of the limitation to BS antennas, non-linear techniques, for example, dirty paper coding [5], vector perturbation [6] or reduced lattice-aided method [7] perform better with higher complexity. In massive MIMO system however, [2] demonstrated that when antenna number on one BS approaches infinity, simple linear precoders such as MF, ZF or MMSE could be optimal. Following sections will focus on

linear precoders and their performance with the aid of optimal ordering (V-BLAST) algorithm.

#### 3.1 Basic Precoding

Basic linear precoding techniques include MF, ZF and MMSE. With perfect knowledge of CSI, estimated transmit signal using MRC (matched filtering in uplink) can be expressed as according to [4]:

$$\hat{x}_{mrc} = G^H y = G^H (\sqrt{\rho} G x + n) \quad (11)$$

Where  $G$  is the reverse link of propagation matrix denoted in (7) and  $\rho$  is the transmitted power. Then the  $k$ th estimated transmit signal can be expanded as:

$$\hat{x}_{mrc} = \sqrt{\rho} \|g_k\|^2 x_k +$$

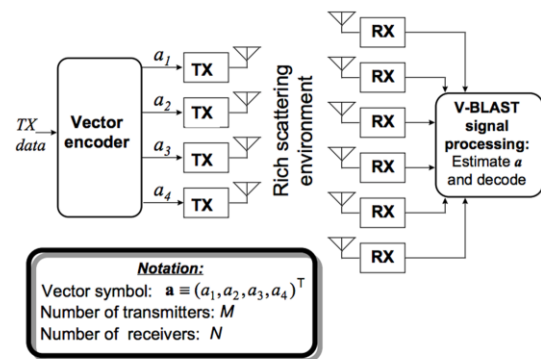


Figure 2: Illustration of V-BLAST System

$$\sqrt{\rho} \sum_{i \neq k}^K g_k^H g_i x_i + g_k^H n \quad (12)$$

Since the single-cell situation is considered here, the resulting expansion is a summation of three terms: the first term explains the desired signal for detection; the second term represents the intra-cell interference between adjacent antennas in same BS; the third term is noise added during transmission. According to (7),  $G \sim \mathcal{CN}(0, \beta)$  and since noise is assumed  $n \sim \mathcal{CN}(0, 1)$ , signal-to-interference-noise ratio (SINR) with MRC is expressed as

$$SINR_k = \frac{\rho \|g_k\|^4}{\rho \sum_{i \neq k}^K |g_k^H g_i|^2 + \|g_k\|^2} = \frac{\rho \|g_k\|^2}{\rho \sum_{i \neq k}^K |\bar{g}_i|^2 + 1} \quad (13)$$

From (7) and (8), when the number of antennas on one BS is much higher than 1 ( $M \gg 1$ ), (13) can be simplified as

$$SINR_k \approx \frac{\rho^M \beta_k}{\rho \sum_{i \neq k}^K |\bar{g}_i|^2 + 1} \quad (14)$$

Thus, when M becomes larger and approaches infinity, the SINR will approach to infinity as well.

For ZF precoding, the estimated transmit signal would be expressed as

$$\hat{x}_{zf} = (G^H G)^{-1} G^H y = \sqrt{\rho} x + (G^H G)^{-1} G^H n \quad (15)$$

When the number of antenna one BS is much larger than 1 ( $M \gg 1$ ), the estimated transmit signal of MRC and ZF are approximated with (8) and (15):

$$\hat{x}_{zf} = (G^H G)^{-1} G^H y \approx \frac{1}{M} D_\beta^{-1} G^H y \approx \hat{x}_{mrc} \quad (16)$$

Compared to MRC and ZF, MMSE usually has a better performance since the precoding scheme include the presence of noise during transmission. The estimated transmit signal for MMSE is defined as

$$\hat{x}_{mmse} = (G^H G + \frac{1}{\rho} I_K)^{-1} G^H y \quad (17)$$

In practical simulation, the  $1/\rho$  term is replaced with relative SNR value in channel matrix for each column vector, thus accounts for the inclusion of noise in estimation.

### 3.2 V-BLAST Algorithm with optimal ordering

V-BLAST algorithm was first proposed in [9] and can be illustrated as Fig. 2. Transmitted data are demultiplexed through vector encoder into several data sub-streams and propagates through rich scattering environment to received antennas. The received signals will be processed with V-BLAST to estimate transmitted signal and decode to obtain the received data. All data streams in V-BLAST follow QAM signal constellation.

Precoding schemes such as ZF and MMSE exploit linear nulling vectors to compensate the effect of channel matrix and noise during transmission. However, these two methods do not consider the possible interference impact between antennas to signal estimation. In V-BLAST, symbol cancellation is employed to detect the interferers and subtract the interference effect from original received signal vector. Thus, optimal detection ordering to determine interferer locations is significant with V-BLAST.

To start with, the estimated transmit signals can be expressed in terms of nulling vector  $W$  and  $k$ th received signal  $y$  as

$$\hat{x}_k = Q(w_k^T y_k) \quad (18)$$

Where  $Q(\cdot)$  represents quantization with signal constellation strategy in use. Besides, according to (15) and (17), the nulling vector for ZF and MMSE are expressed as

$$W_{zf} = (G^H G)^{-1} G^H \quad (19)$$

$$W_{mmse} = (G^H G + \frac{1}{\rho} I_K)^{-1} G^H \quad (20)$$

From [9], with ordered set as  $S \equiv \{k_1, k_2, \dots, k_i, \dots, k_{N_t}\}$ , then the full V-BLAST algorithm can be described with a recursion process. With initial nulling vector,  $k_1$  would be

$$k_1 = \text{argmin}_j \|(w_1)_j\|^2 \quad (21a)$$

The  $i$ th recursion process following is defined as:

$$\hat{x}_{k_i} = Q(w_{k_i}^T y_{k_i}) \quad (21b)$$

$$y_{i+1} = y_i - \hat{x}_{k_i} (H)_{k_i} \quad (21c)$$

$$w_{i+1} = w_{k_i}^- \quad (21d)$$

$$k_{i+1} =$$

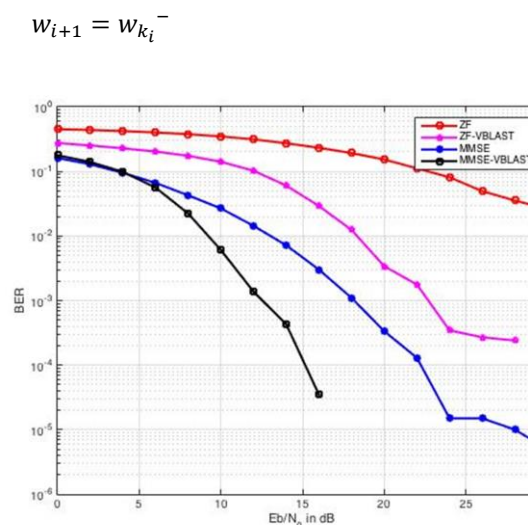


Figure 3: BER Performance for Four Different Precoding Schemes When  $M=K=100$ , Number of Realizations is 100,000 with QPSK Modulation



$$\operatorname{argmin}_{j \notin \{k_1, k_2, \dots, k_i\}} \left| (w_{i+1})_j \right|^2 \quad (21e)$$

$$i \leftarrow i + 1 \quad (21f)$$

Where  $(w_i)_j$  denotes the  $j$ th column of the nulling vector  $w_i$ , and  $w_{k_i}$  in (21d) denotes that the  $k_1, k_2, \dots, k_i$  column of the nulling vectors should be turned to zero after  $i$ th recursion because of symbol cancellation in (21c). The location of optimal ordering is found through (21e), where the minimum interference is achieved in the rest of nulling vectors.

According to Cauchy-Schwartz equality, post-detection SNR will decrease with the increase of rows in channel matrix  $H$ , or the number of antennas equipped on one BS. Besides, the optimal ordering allows for simpler computation because of proceeding symbol cancellation in recursion. When pure nulling is used, the orthogonality to  $M - 1$  rows of channel matrix is required on every nulling vector. With optimal ordering,  $M - 1$  rows will be further reduced to  $M - i$  rows in requirement.

### 3.3 Results

As discussed in [10], precoding performance is associated with the received user power. The case of unequal transmit power, or resource allocation strategy will be discussed in Section 4. This simulation will focus on single-cell signal propagation with equal received user power, which the powers between all links are same and fixed. The multiple antennas on one BS are considered as single antenna array to operate, and the discussion on distributed antenna arrays with possible simplified performance approximations is illustrated by [11] and [12].

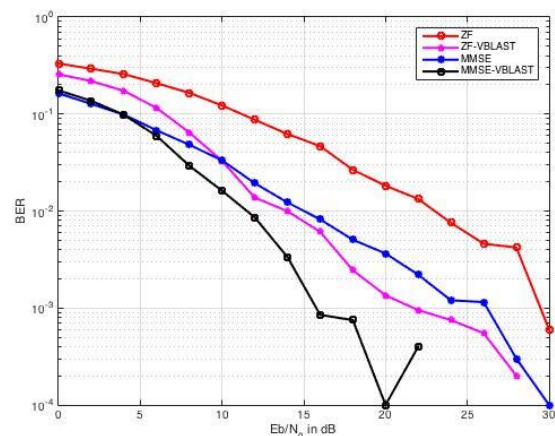
Another assumption is transmission channel to be i.i.d fast fading Rayleigh channel. The channel is memoryless with flat frequency response; thus, current output or estimation is based on current input signal. Furthermore, the received signal is considered primarily composed of desired signal, noise and interference between antennas in one channel. Co-channel interference is assumed low enough to omit in simulation. Noise in presence is set as additive white Gaussian noise (AWGN) with  $n \sim \mathcal{CN}(0,1)$  as denoted in (1).

With perfect knowledge of CSI, the channel matrix  $H$  and nulling vector  $W$  can be obtained. With (19), the nulling vector for ZF precoding is expressed with Moore-Penrose pseudoinverse as  $W_{zf} = G^+$ . For MMSE precoding, since the energy in transmitted signal is normalized, the term explaining for noise in (20) has been replaced with  $1/SNR$ , where SNR is expressed with  $E_b/N_0$  and signal levels.

The four precoding schemes been put into simulation are: ZF, ZF with V-BLAST, MMSE, and MMSE with V-BLAST. Figure 3 and Figure 4 illustrates the bit-error-rate (BER) performance of the four precoding schemes for massive MIMO and simple MIMO system respectively. Both figures indicate that precoding with V-BLAST and optimal ordering generally have better transmission performance than pure nulling methods.

Figure 3 shows the critical results under QPSK modulation for the four precoding schemes. The number of realizations, or bits transmitted is set as 100,000 in simulation. The number of antennas equipped on one BS is 100 and links to same number of user terminals. Since the figure is plotted on a log scale for BER, the absence of results is because the BER rate for MMSE with V-BLAST falls to zero at high SNR value. At low SNR, the BER difference among the four precoding schemes is less than 10dB. However, with the increasing SNR, BER performance of ZF experiences a modest increase, while other three methods have a sharp slope. The MMSE methods is expected to perform better because it takes into consideration the effect of AWGN in channel. Further, the introduction of V-

Figure 4: BER Performance for Four Different Precoding Schemes When  $M=K=8$ , Number of Realizations is 10,000. V-BLAST greatly improves the performance of ZF but cannot be compared to



MMSE. MMSE with V-BLAST has the best performance and able to achieve zero BER in the mid of SNR range.

Figure 4 shows similar simulation under a  $8 \times 8$  MIMO system with the number of realizations equaling 10,000. The performance difference among four linear precoding schemes, however, does not seem to be as large as that in massive MIMO system. The performance of ZF with V-BLAST is almost as same as MMSE. Similarly, as Figure 3, MMSE with V-BLAST precoding still have best performance but some singular values appear at high SNR value. Therefore, linear precoding schemes in conventional

MIMO systems do not have apparent differences between different methods like what displayed in massive MIMO system. More complex and accurate non-linear precoding schemes are used in MIMO system instead, as proposed in [5] [6] [7].

### 3.4 System Complexity

Another issue to discuss in system implementation is complexity. Floating point operations (FLOPS) are discussed in [13] in detail as a measurement of complexity. This part will compare the four precoding techniques in simulation.

For simple ZF linear combiners, (19) shows that its complexity relies on  $(G^H G)$  term. This Hermitian structure does not require any computation on the lower triangle part of the two vectors, thus only  $0.5K(K+1)$  different entries would be evaluated. Since each evaluated element requires for further  $M$  multiplications and  $(M-1)$  summations, the resulting complexity of  $(G^H G)$  term would be

$$0.5MK(K+1) + 0.5(M-1)K(K+1) = MK^2 + MK - 0.5K^2 - 0.5K \quad (22)$$

With the total nulling vector  $(G^H G)^{-1}G^H$  in simple ZF, the multiplication with  $G^H$  required is  $K^2M$  more. Then, the nulling vector should be multiplied by received signal to obtain the estimation for transmit signal, thus the extra multiplication required would be  $MK$ . As a result, the total system complexity expressed by the FLOPS of ZF combiner is

$$FLOPS_{zf} = 0.5K^3 + 1.5K^2 + 1.5MK^2 + 1.5MK \quad (23)$$

For simple MMSE precoding, the extra complexity comes from the noise vectors. According to (20), the  $I_K$  will contribute to an extra  $K^2$  multiplication, thus

$$FLOPS_{mmse} = 0.5K^3 + 2.5K^2 + 1.5MK^2 + 1.5MK \quad (24)$$

With the presence of V-BLAST algorithm, the complexity of simple ZF and MMSE combiners would be multiplied by the number of iterations in the recursion process. For both cases, the number of iterations would be  $(K-1)$ . Then, at the detection stage after symbol cancellation, the complexity will be increased with  $M$  multiplications. Besides, the initial ordering would require for  $MK$  extra multiplications. Thus for the two cases, system complexity would be expressed as

$$FLOPS_{zf-vblast} = FLOPS_{zf} + M + MK \quad (25)$$

$$FLOPS_{mmse-vblast} = FLOPS_{mmse} + M + MK \quad (26)$$

Table 1 summarizes the calculations for the complexity.

Table 1: COMPLEXITY CALCULATIONS

Technique	Complexity
ZF	$0.5K^3 + 1.5K^2 + 1.5MK^2 + 1.5MK$
MMSE	$0.5K^3 + 2.5K^2 + 1.5MK^2 + 1.5MK$
V-BLAST with ZF	$0.5K^3 + 1.5K^2 + 1.5MK^2 + 2.5MK + M$
V-BLAST with MMSE	$0.5K^3 + 2.5K^2 + 1.5MK^2 + 2.5MK + M$

With the massive MIMO system in simulation, where  $M = K = 100$ , the number of multiplications are 2,030,000 for simple ZF combiner; 2,040,000 for simple MMSE combiner; 2,040,100 for V-BLAST with ZF; 2,050,100 for V-BLAST with MMSE precoding scheme. In practice, the four precoding methods take around 9500 seconds to simulate.

### 4. Pilot contamination

Current MIMO system uses frequency-duplex division (FDD), where uplink and downlink transmissions have separate carrier frequencies. As discussed in Section 3, precoding and interference detection requires for perfect knowledge of CSI. The channel estimation with FDD in uplink training can be obtained through sending different pilot sequence. However, downlink channel estimation essentially requires the feedback CSI from different users after sending pilot signals. The downlink processing time in FDD depends on the number of antennas equipped in BS, therefore massive MIMO system usually employs time-duplex division (TDD) in terms of time consumption.

TDD allows for same carrier frequency for uplink and downlink through allocating different time slots. Thus on the basis of channel reciprocity, CSI estimation is only required for uplink and the estimation can be applied to downlink channel. [3] discussed a TDD protocol which first allows for synchronous sending of uplink data then pilot sequences. BSs can estimate CSI with data signal detection and apply the estimation to beamforming vectors for downlink. However, with the constraints on channel coherence time, pilot contamination can arise from the loss of orthogonality in pilot sequences for neighboring cells. Following section will discuss the effect of pilot contamination and

relative mitigation methods with linear uplink receivers.

### 4.1 Pilot Contamination Effect

Precoding schemes discussed in Section 3 consider SINR under single-cell situation. The multi-cell contamination can be illustrated by Fig.5. The SINR of simple MRC precoding defined by (13) and (14) with single-cell should be modified in terms of pilot contamination interference. Hence if the propagation is carried for  $L$  cells, then the estimated signal in  $l$ th cell would be modified with (11) as according to [4]

$$\hat{x}_l = \hat{G}_{ll}^H y_l = (\sum_{j=1}^L G_{lj} + \frac{1}{\sqrt{\rho_p}} W_l)^H (\sqrt{\rho} \sum_{i=1}^L G_{li} x_i + n_l) \quad (27)$$

Where the subscript  $l$  denotes the received signal, transmit signal or noise on the  $l$ th cell. The received would include the pilot contamination contributed by signals in all neighboring cells as well as the desired signal at local cell. The channel matrix includes the nulling vector on local cell in terms of pilot transmit power  $\rho_p$  and interference channel from all other cells.

The expansion of (27) with respect to the number of antennas on one BS is shown as

$$\frac{\hat{x}_l}{M} = \sqrt{\rho} \sum_{i=1}^L \sum_{j=1}^L \frac{G_{lj}^H G_{li}}{M} x_i + \sum_{j=1}^L \frac{G_{lj}^H n_l}{M} + \frac{1}{\sqrt{\rho_p}} \frac{W_l^H n_l}{M} + \sqrt{\frac{\rho}{\rho_p}} \sum_{i=1}^L \frac{W_l^H G_{li}}{M} x_i \quad (28)$$

With the number of antennas  $M$  goes larger and approaches infinity, (7) and (8) could be derived. Then according to [14]

$$\frac{G_{lj}^H G_{li}}{M} = D_{\beta_{lj}}^{1/2} \left( \frac{H_{lj}^H H_{li}}{M} \right) D_{\beta_{li}}^{1/2} \quad (29)$$

The substitution of (8) and (29) to (28) yields

$$\frac{\hat{x}_l}{M} \approx \sqrt{\rho} \sum_{i=1}^L D_{li} x_i \quad (30)$$

Since the  $D_{li}$  is a diagonal matrix comprised of fading coefficients  $\beta$  for pathloss and fading, then signal-to-interference (SIR) for the  $k$ th element of the processed signal becomes

$$SIR_k = \frac{\beta_{lk}^2}{\sum_{i \neq k} \beta_{ik}^2} \quad (31)$$

Therefore, the signal component would be proportional to the second law of large scale fading coefficients in local cell, while interference due to pilot contamination is proportional to the summation of the square of fading coefficient in other neighboring cells. The SIR derived in (31) is independent of either received power or pilot transmit power. The independence is in accordance with the fundamentals of pilot contamination, as it is

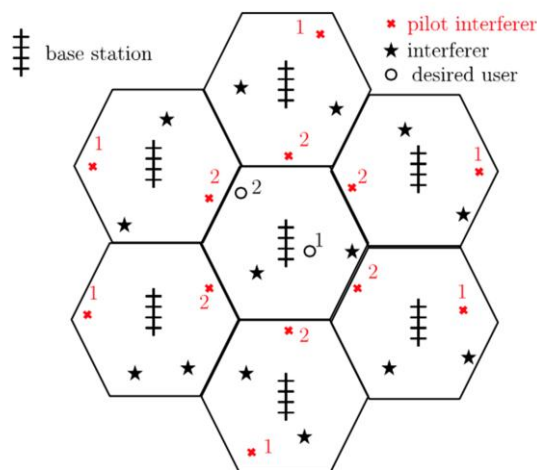


Figure 5: Illustration of Multi-cell Pilot Contamination only limited by the inter-cell interference.

Besides, SIR is independent of frequency since slow fading  $\beta$  is frequency independent. The SIR value is also independent of the absolute cell size, as proved in [14]. As a result, the cell size does not affect the throughput per terminal.

Considering single-cell SINR derived in (13), for MRC precoding scheme, the desired signal on denominator is proportional to the square of fading coefficient as well as the inter-cell interference demonstrated in (31). The noise component terms in (13) has less impact to the entire SINR. Consequently, the dominant impairment comes from pilot contamination rather than noise added to channel during propagation.

Pilot contamination persists existing due to pilot reuse. With the limitation to channel and pilot signal dimensionality, using different pilot sequences for neighboring cells do not suppress the problem. Current mitigation techniques will be reviewed in following section.

### 4.2 Mitigating Pilot Contamination

One mitigation approach proposed by [14] is frequency reuse in propagation or reduce the number of non-orthogonal pilot sequences by constraining the number of users. However, frequency reuse is not

an effective method as simultaneous links to different users is difficult to achieve.

TDD system described in [14] allows for synchronous pilot sequences to be transmitted by all users. To mitigate the pilot contamination, [15] and [16] proposed time-shifted or asynchronous protocols. Fig. 6 can depict a possible pilot sequence

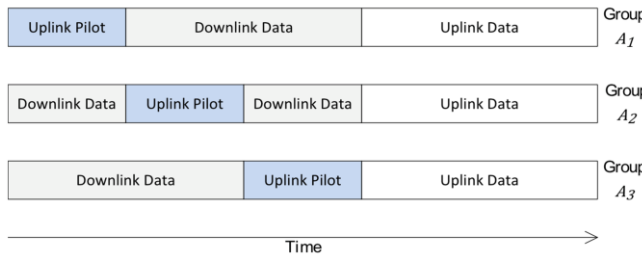


Figure 6: Illustration of Asynchronous Pilot Sequence

arrangement.

The cells are partitioned to three groups in Fig. 6. In each group, the uplink pilot signal does not interfere with pilot intervals from other groups. However, the interference occurs between pilot signals and downlink data. Therefore, transmissions of the pilot signals in non-overlapping times can prevent pilot contamination since the pilot have mutually exclusive sequence manner. When non-orthogonality is prevented, pilot corruption arises from powerful downlink signals in neighboring BSs. Since the mitigation of pilot contamination is not clear, heuristic analysis is performed in [15] and [16].

Then for the uplink training, according to Fig. 1, uplink signals are transmitted simultaneously. Then the received signal with time-shifted frames for the  $l$ th cell can be expressed as

$$Y_l = \sqrt{\rho_r \tau} \Psi_l P_u^{1/2} H_{ll} + \sum_{j=1, j \neq l}^L \sqrt{p_f \gamma_{jl}} D_j G_{jl} + W_l \quad (32)$$

Where for uplink transmission,  $Y_l \in \mathbb{C}^{1 \times M}$  is the received signal for  $M$  antennas at the  $l$ th cell.  $\rho_r$  denotes the average pilot transmitted power by users.  $\Psi_l \in \mathbb{C}^{1 \times K}$  denotes the pilot sequence in the  $l$ th cell.  $\tau = \beta_l K$  where  $\beta_l$  denotes the large scale fading coefficients and  $K$  is the number of users.  $H_{ll} \in \mathbb{C}^{K \times M}$  denotes channel matrix on the  $l$ th cell. In the second term,  $p_f$  representing average downlink data power and  $\gamma_{jl}$  denotes the large scale fading coefficients from other BSs to desired cell.  $W_l \in \mathbb{C}^{K \times M}$  in the third term denotes noise vectors at the  $l$ th cell. The time-shifted method will affect the first term.

In addition, modified precoding schemes are well discussed in [17] - [19] to mitigate pilot contamination. According to the distributed precoding scheme for single-cell proposed by [17], the summation of the squared error from both users in local cell and interference in neighboring cells are minimized. In the optimal objective function, a weighting vector is multiplier by the interference as well. It shows that the MMSE-based precoding schemes have better sum rate performance compared to ZF methods in multi-cell MIMO systems and the advantages become larger when more antennas are equipped on one BS.

In terms of massive MIMO system, [18] and [19] employ adaptive MMSE filtering. The derivation of the MMSE filter is a time-dependent recursion process. Assumed with perfect knowledge of received signal and channel matrix information, the MMSE filter initialization is achieved by minimizing the absolute squared error for transmit signal estimation. Then with the time index denoting resources spending on uplink pilot training data, the MMSE filter on current index is determined with the filter information on last index, pilot sequences and received signal on current index. [18] indicates a 10dB SINR improvement with this recursive MMSE filtering than conventional matched filtering under same pilot contamination conditions.

## 5. Hardware impairments

For system model analysis in above Sections, signals are assumed to propagate with perfect transceivers. In practice, amplifier non-linearities, quantization errors [20] and phase noise [22] can occur with non-ideal hardwares and result in the limited system capacity in high-power situation. Since one benefit of massive MIMO system is the introduction of low-cost hardware components, the impairments are exacerbated. Analog and digital signal processing can compensate the impairments to some extent, however the impact cannot be thoroughly removed. A low value of peak-to-average ratio (PAPR) can mitigate the effect of amplifier non-linearities. Phase noise is significant in deciding the lower bounds of total sum rate, thus common compensation is achieved with proper uplink receiver [22].

Two critical impacts on signal propagations are: mismatch between ideal and practical transmit signals; distortion of received signals. Hence for a downlink transmission, modification can be made to (1) as

$$y = \sqrt{\rho} \mathbf{H}(x + \eta_t) + \eta_r + n \quad (33)$$



Where  $\eta_t \in \mathbb{C}^{M \times 1}$  and  $\eta_r \in \mathbb{C}^{M \times 1}$  denotes the transceiver impairments on transmitter and receiver terminals respectively. According to [20], the impairment parameters are assumed depending on channel matrix  $\mathbf{H}$  but not on transmit signals. Besides, they are modeled with Gaussian distribution where the variances are determined by transceiver conditions.

The compensation to phase noise is conducted with time-reversal MRC (TR-MRC) schemes to uplink receiver. According to [22], phase noise exists in oscillator leads to signal distortion on reception end. The basic idea of TR-MRC is to inject two different complex terms to compensate the phase noise in different coherence intervals under asynchronous operation. With phase noise, [22] illustrates that the sum rate is likely to decay with increasing duration of data phase rather than approaching infinity like ideal transceiver. TR-MRC can remove part of the decaying effect but works better with non-synchronous operation, thus independent phase noise resources are suggested in the practical system setup.

## 6. Conclusions

This paper describes massive MIMO system from the perspective of information theory, precoding schemes, pilot contamination and practical considerations like hardware impairments. Equipped with a large number of antenna arrays on one BS, both energy and spectral efficiency of system are significantly improved compared with conventional MIMO system. Present research topics include the hardware implementations, management of interference, resource allocation etc. in order to apply the benefits of massive MIMO system to practice.

Possible challenges on massive MIMO system are discussed in [3] regarding to both theoretical and implementation issues. Apart from pilot contamination and hardware impairments, the non-orthogonality due to larger antenna correlation coefficients than i.i.d. assumptions, increased computational costs and the configuration of proper antenna array requires more research on system models. The major application challenge discussed in [3] deals with heterogeneous networks (HetNets), as small cells with massive MIMO systems can ensure a satisfactory energy efficiency and quality-of-service expectations for user crowded area [21]. Interference between massive MIMO systems and small cells, the deployment of millimeter wave (MMW) techniques in terms of HetNets requires more studies in further research.

## Acknowledgments

The author would like to thank Prof. K. Sowerby with University of Auckland for valuable comments and suggestions during the project.

## References

- [1] E.G. Larsson, O. Edfors, F. Tufvesson, and T.L. Marzetta, "Massive MIMO for next generation wireless systems", *IEEE Communications Magazine*, vol.52, no.2, pp. 186-195, Feb. 2014
- [2] F. Rusek, D. Persson, B.K. Lau, E.G. Larsson, T.L. Marzetta, O. Edfors, and F. Tufvesson, "Scaling up MIMO: Opportunities and challenges with very large arrays", *IEEE Signal Processing Magazine*, vol. 30, no. 1, pp. 40-46, Jan. 2013
- [3] L. Lu, G. Y. Li, A. L. Swindlehurst, A. Ashikhmin, and R. Zhang, "An overview of massive MIMO: Benefits and challenges", *IEEE Journal of Selected Topics on Signal Processing*, vol.8, no.5, pp. 742-758, Oct. 2014
- [4] E. G. Larsson, "Very large MIMO systems: Opportunities and challenges", Mar. 2012 [Online] Available at: [https://www.kth.se/polopoly\\_fs/1.303070!/Menu/genera/column-content/attachment/Large\\_MIMO.pdf](https://www.kth.se/polopoly_fs/1.303070!/Menu/genera/column-content/attachment/Large_MIMO.pdf)
- [5] M. Costa, "Writing on dirty paper", *IEEE Trans. Inf. Theory*, vol. IT-29, no. 3, pp. 439-441, May 1983
- [6] B. M. Hochwald, C. B. Peel, and A. L. Swindlehurst, "A vector-perturbation technique for near-capacity multiantenna communication-part II: Perturbation", *IEEE Trans. Communication*, vol. 53, no. 5, pp. 537-544, May 2005
- [7] Z. Keke, R. C. de Lamare, and M. Haardt, "Low-complexity lattice reduction-aided channel inversion methods for large multi-user MIMO systems", 2012 Conference Record of Forty Sixth Asilomar Conference on Signals, Systems and Computers, pp. 463-467, Nov. 2012
- [8] H. Q. Ngo, E.G. Larsson, and T.L. Marzetta, "Energy and spectral efficiency of very large multiuser MIMO systems", *IEEE Trans. Communication*, vol. 61, no. 4, pp. 1436-1449, Apr. 2013
- [9] P. W. Wolniansky, G. J. Foschini, G. D. Golden, and R. A. Valenzuela, "V-BLAST: An architecture for realizing very high data rate over the rich-scattering wireless channel", 1998 [Online] Available at: <http://www.ee.columbia.edu/~jiantan/E6909/wolnianskyandfoschini.pdf>
- [10] K. A. Alnajar, P. J. Smith, and G. K. Woodward, "Low complexity V-BLAST for massive MIMO", 2014 Australian Communications Theory Workshop (AusCTW), pp.22-26, Feb. 2014
- [11] D. A. Basnayaka, P. J. Smith, and P. A. Martin, "Performance analysis of macrodiversity MIMO systems with MMSE and ZF receivers in flat Rayleigh fading", *IEEE Trans. Wireless Commun.*, vol. 12, no. 5, pp. 2240-2251, Apr. 2013
- [12] J. Yi, M. K. Varanasi, and L. Jian, "Performance analysis of ZF and MMSE equalizers for MIMO systems: An in-depth study of the high SNR regime", *IEEE Trans. Information Theory*, vol. 57, no. 4, pp. 2008-2026, Apr. 2011
- [13] R. Hunger, "Floating point operations in matrix-vector calculus", Technical report V1.3, Munich University of Technology, 2007 [Online] Available at: <https://mediatum.ub.tum.de/doc/625604/625604.pdf>

- [14] T. L. Marzetta, "Noncooperative cellular wireless with unlimited numbers of base station antennas", *IEEE Trans. Wireless Commun.*, vol. 9, no. 11, pp. 3590-3600, Nov. 2010
- [15] W. A. W. M. Mahyiddin, A. M. Philippa, and P. J. Smith, "Pilot contamination reduction using time-shifted pilots in finite massive MIMO systems", *2014 IEEE 80<sup>th</sup> Vehicular Technology Conference*, pp. 1-5, Spet. 2014
- [16] K. Appaiah, A. Ashikmin, and T. L. Marzetta, "Pilot contamination reduction in multi-user TDD systems", in *Proc. IEEE Int. Conf. Commun. (ICC)*, Jun. 2012
- [17] J. Jose, A. Ashikhmin, T. Marzetta, and S. Vishwanath, "Pilot contamination and precoding in multi-cell TDD systems", *IEEE Trans. Commun.*, vol. 10, no. 8, pp. 2640-2651, 2011
- [18] N. Krishnan, R. D. Yates, and N. B. Mandayam, "Uplink linear receivers for multi-cell multiuser MIMO with pilot contamination: Large system analysis", *IEEE Trans. Wireless Commun.*, vol. 13, no. 8, Aug. 2014
- [19] N. Krishnan, R. D. Yates, and N. B. Mandayam, "Cellular systems with many antennas: Large system analysis under pilot contamination", in *Proc. 50<sup>th</sup> Annu. Allerton Conf. Commun., Control, Comput.*, Jun. 2012, pp. 1220-1224
- [20] E. Bjornson, J. Hoydis, M. Kountouris, and M. Debbah, "Massive MIMO systems with non-ideal hardware: Energy efficiency, estimation, and capacity limits", *IEEE Trans. Information Theory*, vol. 60, no. 11, pp. 7112-7139, Nov. 2014
- [21] E. Bjornson, M. Kountouris, and M. Debbah, "Massive MIMO and small cells: Improving energy efficiency by optimal soft-cell coordination", *International Conference on Telecommunications*, May 2013
- A. Pitarokoilis, S. K. Mohammed, and E. G. Larsson, "Uplink performance of time-reversal MRC in massive MIMO systems subject to phase noise," *IEEE Trans. Wireless Commun.*, vol. 14, pp. 711-723, 2015